EUROPEAN ORGANIZATION FOR NUCLEAR RESEARCH

CERN–PPE/94–31

23 February 1994

Improved Measurements of Cross Sections and Asymmetries at the Z^0 Resonance

DELPHI Collaboration

Abstract

During the 1992 running period of the LEP e^+e^- collider, the DELPHI experiment accumulated approximately 24 pb^{-1} of data at the Z^0 peak. The decays into hadrons and charged leptons have been analysed to give values for the cross sections and leptonic forward-backward asymmetries which are significantly improved with respect to those previously published by the DELPHI collaboration. Incorporating these new data, more precise values for the Z^0 resonance parameters are obtained from model–independent fits. The results are interpreted within the framework of the Standard Model, yielding for the top quark mass $m_t = 157^{+36}_{-48}(expt.)^{+19}_{-20}(Higgs)$ GeV, and for the effective mixing angle $\sin^2\theta^{lept}_{eff} = 0.2328 \pm 0.0013(expt.)^{+0.0001}_{-0.0003}(Higgs)$, where $(Higgs)$ represents the variation due to Higgs boson mass in the range 60 to 1000 GeV, with central value 300 GeV.

(To be submitted to Nucl. Phys. B)

P.Abreu[20], W.Adam[7], T.Adye[37], E.Agasi[30], I.Ajinenko[42], R.Aleksan[39], G.D.Alekseev[14], P.P.Allport[21], S.Almehed[23], F.M.L.Almeida[47], S.J.Alvsvaag[4], U.Amaldi[7], A.Andreazza[27], P.Antilogus[24], W-D.Apel[15], R.J.Apsimon[37], Y.Arnoud[39], B.Åsman[44], J-E.Augustin[18], A.Augustinus[30], P.Baillon[7], P.Bambade[18], F.Barao[20], R.Barate[12], G.Barbiellini[46], D.Y.Bardin[14], G.J.Barker[34], A.Baroncelli[40], O.Barring[7], J.A.Barrio[25], W.Bartl[50], M.J.Bates[37], M.Battaglia[13], M.Baubillier[22], K-H.Becks[52], M.Begalli[36], P.Beilliere[6], K.Belous[42], P.Beltran[9], A.C.Benvenuti[5], M.Berggren[41], D.Bertrand[2], F.Bianchi[45], M.Bigi[45], M.S.Bilenky[14], P.Billoir[22], J.Bjarne[23], D.Bloch[8], J.Blocki[51], S.Blyth[34], V.Bocci[38], P.N.Bogolubov[14], T.Bolognese[39], M.Bonesini[27], W.Bonivento[27], P.S.L.Booth[21], G.Borisov[42], C.Bosio[40], B.Bostjancic[43], S.Bosworth[34], O.Botner[48], B.Bouquet[18], C.Bourdarios[18], T.J.V.Bowcock[21], M.Bozzo[11], S.Braibant[2], P.Branchini[40], K.D.Brand[35], R.A.Brenner[13], H.Briand[22], C.Bricman[2], L.Brillault[22], R.C.A.Brown[7], J-M.Brunet[6], L.Bugge[32], T.Buran[32], A.Buys[7], J.A.M.A.Buytaert[7], M.Caccia[27], M.Calvi[27], A.J.Camacho Rozas[41], R.Campion[21], T.Camporesi[7], V.Canale[38], K.Cankocak[44], F.Cao[2], F.Carena[7], P.Carrilho[47], L.Carroll[21], R.Cases[49], C.Caso[11], M.V.Castillo Gimenez[49], A.Cattai[7], F.R.Cavallo[5], L.Cerrito[38], V.Chabaud[7], A.Chan[1], Ph.Charpentier[7], J.Chauveau[22], P.Checchia[35], G.A.Chelkov[14], L.Chevalier[39], P.Chliapnikov[42], V.Chorowicz[22], J.T.M.Chrin[49], V.Cindro[43], P.Collins[34], J.L.Contreras[18], R.Contri[11], E.Cortina[49], G.Cosme[18], F.Couchot[18], H.B.Crawley[1], D.Crennell[37], G.Crosetti[11], J.Cuevas Maestro[33], S.Czellar[13], E.Dahl-Jensen[28], J.Dahm[52], B.Dalmagne[18], M.Dam[32], G.Damgaard[28], E.Daubie[2], A.Daum[15], P.D.Dauncey[7], M.Davenport[7], J.Davies[21], W.Da Silva[22], C.Defoix[6], G.Della Ricca[46], P.Delpierre[26], N.Demaria[34], A.De Angelis[7], H.De Boeck[2], W.De Boer[15], S.De Brabandere[2], C.De Clercq[2], M.D.M.De Fez Laso[49], C.De La Vaissiere[22], B.De Lotto[46], A.De Min[27], L.De Paula[47], H.Dijkstra[7], L.Di Ciaccio[38], F.Djama[8], J.Dolbeau[6], M.Donszelmann[7], K.Doroba[51], M.Dracos[8], J.Drees[52], M.Dris[31], Y.Dufour[7], F.Dupont[12], D.Edsall[1], R.Ehret[15], T.Ekelof[48], G.Ekspong[44], M.Elsing[52], J-P.Engel[8], N.Ershaidat[22], M.Espirito Santo[20], D.Fassouliotis[31], M.Feindt[7], A.Ferrer[49], T.A.Filippas[31], A.Firestone[1], H.Foeth[7], E.Fokitis[31], F.Fontanelli[11], F.Formenti[7], J-L.Fousset[26], S.Francon[24], B.Franek[37], P.Frenkiel[6], D.C.Fries[15], A.G.Frodesen[4], R.Fruhwirth[50], F.Fulda-Quenzer[18], H.Furstenau[7], J.Fuster[7], D.Gamba[45], M.Gandelman[17], C.Garcia[49], J.Garcia[41], C.Gaspar[7], U.Gasparini[35], Ph.Gavillet[7], E.N.Gazis[31], D.Gele[8], J-P.Gerber[8], L.Gerdyukov[42], P.Giacomelli[7], D.Gillespie[7], R.Gokieli[51], B.Golob[43], V.M.Golovatyuk[14], J.J.Gomez Y Cadenas[7], G.Gopal[37], L.Gorn[1], M.Gorski[51], V.Gracco[11], F.Grard[2], E.Graziani[40], G.Grosdidier[18], P.Gunnarsson[44], J.Guy[37], U.Haedinger[15], F.Hahn[52], M.Hahn[44], S.Hahn[52], S.Haider[30], Z.Hajduk[16], A.Hakansson[23], A.Hallgren[48], K.Hamacher[52], G.Hamel De Monchenault[39], W.Hao[30], F.J.Harris[34], V.Hedberg[23], R.Henriques[20], J.J.Hernandez[49], J.A.Hernando[49], P.Herquet[2], H.Herr[7], T.L.Hessing[21], E.Higon[49], H.J.Hilke[7], T.S.Hill[1], S-O.Holmgren[44], P.J.Holt[34], D.Holthuizen[30], P.F.Honore[6], M.Houlden[21], J.Hrubec[50], K.Huet[2], K.Hultqvist[44], P.Ioannou[3], P-S.Iversen[4], J.N.Jackson[21], R.Jacobsson[44], P.Jalocha[16], G.Jarlskog[23], P.Jarry[39], B.Jean-Marie[18], E.K.Johansson[44], M.Jonker[7], L.Jonsson[23], P.Juillot[8], M.Kaiser[15], G.Kalmus[37], F.Kapusta[22], M.Karlsson[44], E.Karvelas[9], S.Katsanevas[3], E.C.Katsoufis[31], R.Keranen[7], B.A.Khomenko[14], N.N.Khovanski[14], B.King[21], N.J.Kjaer[28], H.Klein[7], A.Klovning[4], P.Kluit[30], A.Koch-Mehrin[52], J.H.Koehne[15], B.Koene[30], P.Kokkinias[9], M.Koratzinos[32], K.Korcyl[16], A.V.Korytov[14], V.Kostioukhine[42], C.Kourkoumelis[3], O.Kouznetsov[14], P.H.Kramer[52], M.Krammer[50], C.Kreuter[15], J.Krolikowski[51], I.Kronkvist[23], W.Krupinski[16], K.Kulka[48], K.Kurvinen[13], C.Lacasta[49], C.Lambropoulos[9], J.W.Lamsa[1], L.Lanceri[46], P.Langefeld[52], V.Lapin[42], I.Last[21], J-P.Laugier[39], R.Lauhakangas[13], G.Leder[50], F.Ledroit[12], R.Leitner[29], Y.Lemoigne[39], J.Lemonne[2], G.Lenzen[52], V.Lepeltier[18], T.Lesiak[16], J.M.Levy[8], E.Lieb[52], D.Liko[50], R.Lindner[52], A.Lipniacka[18], I.Lippi[35], B.Loerstad[23], M.Lokajicek[10], J.G.Loken[34], A.Lopez-Fernandez[7], M.A.Lopez Aguera[41], M.Los[30], D.Loukas[9], J.J.Lozano[49], P.Lutz[6], L.Lyons[34], G.Maehlum[15], J.Maillard[6], A.Maio[20], A.Maltezos[9], F.Mandl[50], J.Marco[41], B.Marechal[47], M.Margoni[35], J-C.Marin[7], C.Mariotti[40], A.Markou[9], T.Maron[52], S.Marti[49], C.Martinez-Rivero[41], F.Martinez-Vidal[49], F.Matorras[41], C.Matteuzzi[27], G.Matthiae[38], M.Mazzucato[35], M.Mc Cubbin[21], R.Mc Kay[1], R.Mc Nulty[21], J.Medbo[48], C.Meroni[27], W.T.Meyer[1], M.Michelotto[35], E.Migliore[45], I.Mikulec[50], L.Mirabito[24], W.A.Mitaroff[50], G.V.Mitselmakher[14], U.Mjoernmark[23], T.Moa[44], R.Moeller[28], K.Moenig[7], M.R.Monge[11], P.Morettini[11], H.Mueller[15], W.J.Murray[37], B.Muryn[16], G.Myatt[34], F.Naraghi[12], F.L.Navarria[5], P.Negri[27], S.Nemecek[10], W.Neumann[52], N.Neumeister[50], R.Nicolaidou[3], B.S.Nielsen[28], P.E.S.Nilsen[4], P.Niss[44], A.Nomerotski[35], A.Normand[34], V.Obraztsov[42], A.G.Olshevski[14], R.Orava[13], K.Osterberg[13], A.Ouraou[39], P.Paganini[18], M.Paganoni[27], R.Pain[22], H.Palka[16], Th.D.Papadopoulou[31], L.Pape[7], F.Parodi[11], A.Passeri[40], M.Pegoraro[35], J.Pennanen[13], L.Peralta[20], H.Pernegger[50], M.Pernicka[50], A.Perrotta[5], A.Petrolini[11], H.T.Phillips[37], G.Piana[11], F.Pierre[39], M.Pimenta[20], S.Plaszczynski[18], O.Podobrin[15], M.E.Pol[17], G.Polok[16], P.Poropat[46], V.Pozdniakov[14], M.Prest[46], P.Privitera[38], A.Pullia[27], D.Radojicic[34], S.Ragazzi[27], H.Rahmani[31], J.Rames[10], P.N.Ratoff[19], A.L.Read[32], M.Reale[52], P.Rebecchi[18], N.G.Redaelli[27], D.Reid[7], P.B.Renton[34], L.K.Resvanis[3], F.Richard[18], J.Richardson[21], J.Ridky[10], G.Rinaudo[45], A.Romero[45], I.Roncagliolo[11], P.Ronchese[35], V.Ronjin[42], L.Roos[12], E.I.Rosenberg[1], E.Rosso[7], P.Roudeau[18], T.Rovelli[5], W.Ruckstuhl[30], V.Ruhlmann-Kleider[39], A.Ruiz[41], K.Rybicki[16], H.Saarikko[13], Y.Sacquin[39], G.Sajot[12], J.Salt[49], J.Sanchez[25], M.Sannino[11], S.Schael[7], H.Schneider[15], M.A.E.Schyns[52], G.Sciolla[45], F.Scuri[46], A.M.Segar[34], A.Seitz[15],

R.Sekulin[37], R.Seufert[15], R.C.Shellard[36], I.Siccama[30], P.Siegrist[39], S.Simonetti[11], F.Simonetto[35], A.N.Sisakian[14], G.Skjevling[32], G.Smadja[24], N.Smirnov[42], O.Smirnova[14], G.R.Smith[37], R.Sosnowski[51], D.Souza-Santos[36], T.Spassov[20], E.Spiriti[40], S.Squarcia[11], H.Staeck[52], C.Stanescu[40], S.Stapnes[32], I.Stavitski[35], G.Stavropoulos[9], K.Stepaniak[51], F.Stichelbaut[7], A.Stocchi[18], J.Strauss[50], J.Straver[7], R.Strub[8], B.Stugu[4], M.Szczekowski[51], M.Szeptycka[51], T.Tabarelli[27], O.Tchikilev[42], G.E.Theodosiou[9], Z.Thome[47], A.Tilquin[26], J.Timmermans[30], V.G.Timofeev[14], L.G.Tkatchev[14], T.Todorov[8], D.Z.Toet[30], A.Tomaradze[2], B.Tome[20], E.Torassa[45], L.Tortora[40], G.Transtromer[23], D.Treille[7], W.Trischuk[7], G.Tristram[6], C.Troncon[27], A.Tsirou[7], E.N.Tsyganov[14], M.Turala[16], M-L.Turluer[39], T.Tuuva[13], I.A.Tyapkin[22], M.Tyndel[37], S.Tzamarias[21], B.Ueberschaer[52], S.Ueberschaer[52], O.Ullaland[7], V.Uvarov[42], G.Valenti[5], E.Vallazza[7], J.A.Valls Ferrer[49], C.Vander Velde[2], G.W.Van Apeldoorn[30], P.Van Dam[30], M.Van Der Heijden[30], W.K.Van Doninck[2], J.Van Eldik[30], P.Vaz[7], G.Vegni[27], L.Ventura[35], W.Venus[37], F.Verbeure[2], M.Verlato[35], L.S.Vertogradov[14], D.Vilanova[39], P.Vincent[24], L.Vitale[46], E.Vlasov[42], A.S.Vodopyanov[14], M.Vollmer[52], M.Voutilainen[13], V.Vrba[10], H.Wahlen[52], C.Walck[44], F.Waldner[46], A.Wehr[52], M.Weierstall[52], P.Weilhammer[7], A.M.Wetherell[7], J.H.Wickens[2], M.Wielers[15], G.R.Wilkinson[34], W.S.C.Williams[34], M.Winter[8], M.Witek[7], G.Wormser[18], K.Woschnagg[48], K.Yip[34], O.Yushchenko[42], A.Zaitsev[42], A.Zalewska[16], P.Zalewski[51], D.Zavrtanik[43], E.Zevgolatakos[9], N.I.Zimin[14], M.Zito[39], D.Zontar[43], R.Zuberi[34], G.Zumerle[35], J.Zuniga[49]

[1] Ames Laboratory and Department of Physics, Iowa State University, Ames IA 50011, USA
[2] Physics Department, Univ. Instelling Antwerpen, Universiteitsplein 1, B-2610 Wilrijk, Belgium
and IIHE, ULB-VUB, Pleinlaan 2, B-1050 Brussels, Belgium
and Faculté des Sciences, Univ. de l'Etat Mons, Av. Maistriau 19, B-7000 Mons, Belgium
[3] Physics Laboratory, University of Athens, Solonos Str. 104, GR-10680 Athens, Greece
[4] Department of Physics, University of Bergen, Allégaten 55, N-5007 Bergen, Norway
[5] Dipartimento di Fisica, Università di Bologna and INFN, Via Irnerio 46, I-40126 Bologna, Italy
[6] Collège de France, Lab. de Physique Corpusculaire, IN2P3-CNRS, F-75231 Paris Cedex 05, France
[7] CERN, CH-1211 Geneva 23, Switzerland
[8] Centre de Recherche Nucléaire, IN2P3 - CNRS/ULP - BP20, F-67037 Strasbourg Cedex, France
[9] Institute of Nuclear Physics, N.C.S.R. Demokritos, P.O. Box 60228, GR-15310 Athens, Greece
[10] FZU, Inst. of Physics of the C.A.S. High Energy Physics Division, Na Slovance 2, CS-180 40, Praha 8, Czechoslovakia
[11] Dipartimento di Fisica, Università di Genova and INFN, Via Dodecaneso 33, I-16146 Genova, Italy
[12] Institut des Sciences Nucléaires, IN2P3-CNRS, Université de Grenoble 1, F-38026 Grenoble, France
[13] Research Institute for High Energy Physics, SEFT, P.O. Box 9, FIN-00014 University of Helsinki, Finland
[14] Joint Institute for Nuclear Research, Dubna, Head Post Office, P.O. Box 79, 101 000 Moscow, Russian Federation
[15] Institut für Experimentelle Kernphysik, Universität Karlsruhe, Postfach 6980, D-76128 Karlsruhe, Germany
[16] High Energy Physics Laboratory, Institute of Nuclear Physics, Ul. Kawiory 26a, PL-30055 Krakow 30, Poland
[17] Centro Brasileiro de Pesquisas Físicas, rua Xavier Sigaud 150, RJ-22290 Rio de Janeiro, Brazil
[18] Université de Paris-Sud, Lab. de l'Accélérateur Linéaire, IN2P3-CNRS, Bat 200, F-91405 Orsay, France
[19] School of Physics and Materials, University of Lancaster, Lancaster LA1 4YB, UK
[20] LIP, IST, FCUL - Av. Elias Garcia, 14-1°, P-1000 Lisboa Codex, Portugal
[21] Department of Physics, University of Liverpool, P.O. Box 147, Liverpool L69 3BX, UK
[22] LPNHE, IN2P3-CNRS, Universités Paris VI et VII, Tour 33 (RdC), 4 place Jussieu, F-75252 Paris Cedex 05, France
[23] Department of Physics, University of Lund, Sölvegatan 14, S-22363 Lund, Sweden
[24] Université Claude Bernard de Lyon, IPNL, IN2P3-CNRS, F-69622 Villeurbanne Cedex, France
[25] Universidad Complutense, Avda. Complutense s/n, E-28040 Madrid, Spain
[26] Univ. d'Aix - Marseille II - CPP, IN2P3-CNRS, F-13288 Marseille Cedex 09, France
[27] Dipartimento di Fisica, Università di Milano and INFN, Via Celoria 16, I-20133 Milan, Italy
[28] Niels Bohr Institute, Blegdamsvej 17, DK-2100 Copenhagen 0, Denmark
[29] NC, Nuclear Centre of MFF, Charles University, Areal MFF, V Holesovickach 2, CS-180 00, Praha 8, Czechoslovakia
[30] NIKHEF-H, Postbus 41882, NL-1009 DB Amsterdam, The Netherlands
[31] National Technical University, Physics Department, Zografou Campus, GR-15773 Athens, Greece
[32] Physics Department, University of Oslo, Blindern, N-1000 Oslo 3, Norway
[33] Dpto. Fisica, Univ. Oviedo, C/P.Jimenez Casas, S/N-33006 Oviedo, Spain
[34] Department of Physics, University of Oxford, Keble Road, Oxford OX1 3RH, UK
[35] Dipartimento di Fisica, Università di Padova and INFN, Via Marzolo 8, I-35131 Padua, Italy
[36] Depto. de Fisica, Pontificia Univ. Católica, C.P. 38071 RJ-22453 Rio de Janeiro, Brazil
[37] Rutherford Appleton Laboratory, Chilton, Didcot OX11 OQX, UK
[38] Dipartimento di Fisica, Università di Roma II and INFN, Tor Vergata, I-00173 Rome, Italy
[39] Centre d'Etude de Saclay, DSM/DAPNIA, F-91191 Gif-sur-Yvette Cedex, France
[40] Istituto Superiore di Sanità, Ist. Naz. di Fisica Nucl. (INFN), Viale Regina Elena 299, I-00161 Rome, Italy
[41] C.E.A.F.M., C.S.I.C. - Univ. Cantabria, Avda. los Castros, S/N-39006 Santander, Spain
[42] Inst. for High Energy Physics, Serpukov P.O. Box 35, Protvino, (Moscow Region), Russian Federation
[43] J. Stefan Institute and Department of Physics, University of Ljubljana, Jamova 39, SI-61000 Ljubljana, Slovenia
[44] Fysikum, Stockholm University, Box 6730, S-113 85 Stockholm, Sweden
[45] Dipartimento di Fisica Sperimentale, Università di Torino and INFN, Via P. Giuria 1, I-10125 Turin, Italy
[46] Dipartimento di Fisica, Università di Trieste and INFN, Via A. Valerio 2, I-34127 Trieste, Italy
and Istituto di Fisica, Università di Udine, I-33100 Udine, Italy
[47] Univ. Federal do Rio de Janeiro, C.P. 68528 Cidade Univ., Ilha do Fundão BR-21945-970 Rio de Janeiro, Brazil
[48] Department of Radiation Sciences, University of Uppsala, P.O. Box 535, S-751 21 Uppsala, Sweden
[49] IFIC, Valencia-CSIC, and D.F.A.M.N., U. de Valencia, Avda. Dr. Moliner 50, E-46100 Burjassot (Valencia), Spain
[50] Institut für Hochenergiephysik, Österr. Akad. d. Wissensch., Nikolsdorfergasse 18, A-1050 Vienna, Austria
[51] Inst. Nuclear Studies and University of Warsaw, Ul. Hoza 69, PL-00681 Warsaw, Poland
[52] Fachbereich Physik, University of Wuppertal, Postfach 100 127, D-42097 Wuppertal 1, Germany

1 Introduction

During 1990 and 1991 energy scans around the position of the Z^0 resonance were performed at LEP. These data have been carefully analysed and, using the precise measurements of the LEP energy [1], the DELPHI collaboration has published accurate determinations of the Z^0 resonance parameters [2].

The analysis of the 1992 data is reported here. All the data were taken at an energy close to the Z^0 peak and therefore add little to the determination of the mass and width of the resonance. However, the large increase in statistics and the reduction of some systematic errors allow significantly improved determinations of the cross sections and leptonic forward–backward asymmetries at the peak.

Following the recommendation of the Working Group on LEP Energy [3] a single centre of mass energy was used for the 1992 data. Each fill was assigned an energy based on the measured magnetic field in a reference magnet. An average of these energies, weighted by the integrated luminosity of each fill, was then calculated and an offset derived from the resonant depolarisation measurements was applied [3]. The result is a value of

$$E_{cms} \quad = \quad 91.280 \pm 0.018 \text{ GeV}.$$

The energy spread of particles in the beams leads to an rms spread of centre-of-mass energies of 51 ± 5 MeV [3]. Small corrections for this effect have been applied to all the cross sections reported here. The data analysed correspond to an integrated luminosity of approximately 24 pb^{-1}.

This paper is organised as follows. Section 2 contains a brief description of the components of the DELPHI detector relevant for this analysis. In Section 3 the luminosity measurement is described and in Section 4 the hadronic event selection and cross section determination. Section 5 contains a description of the event selections, and cross section and forward–backward asymmetry determinations in the channels e^+e^-, $\mu^+\mu^-$ and $\tau^+\tau^-$, as well as the results of an inclusive lepton selection. Section 6 reports on fits to the combined 1990, 1991 and 1992 data of the DELPHI collaboration, and in Section 7 the results are interpreted within the framework of the Standard Model. Section 8 gives a summary of the results.

2 The DELPHI Detector

A detailed description of the DELPHI detector can be found in reference [4]. In the barrel region the trajectories of charged particles in the 1.2 T solenoidal magnetic field are measured using, (in order of increasing distance from the beams) the silicon Microvertex Detector (VD), the Inner Detector (ID), the Time Projection Chamber (TPC) and the Outer Detector (OD). In the forward region track reconstruction is complemented by the drift chambers A and B (FCA and FCB). Electromagnetic energy is measured by the High Density Projection Chamber (HPC) in the barrel and by lead glass detectors (FEMC) in the forward regions. The return yoke of the solenoid is instrumented as a hadron calorimeter (HCAL) and drift chambers for muon identification surround both the barrel (MUB) and forward (MUF) regions. A lead-scintillator calorimeter (SAT) detects Bhabha scattering events at small angle and is used to measure the luminosity. The readout of the detector is triggered by redundant combinations of signals from scintillators, from the tracking chambers and from the calorimeters.

The response of the detector to physics processes was modelled using the simulation program DELSIM [5], which incorporates the resolution, granularity and efficiency of the

detector components. Simulated data were passed through the same reconstruction and analysis chains as the real data.

3 The Luminosity Measurement

The luminosity measurement in 1992 was based on the Small Angle Tagger (SAT). This calorimeter detected Bhabha scattering events in the polar angle range 43 to 135 mrad. The acceptance was defined by an accurately machined mask in front of one of the calorimeters. The original lead mask was replaced for part of the 1992 running by one of tungsten, which could be machined to tighter tolerances. In addition the new mask extended to smaller radii, thus preventing electrons from entering the calorimeter under the ring mask. An additional lead mask covers the $\pm 15^\circ$ in azimuth around the vertical junction of the calorimeter half-barrels. A lead cylinder prevented electrons entering the unmasked calorimeter at small angles, and so the spurious high energy deposits seen previously [2] were eliminated. The luminosity trigger was a coincidence of energy depositions of more than 12 GeV coplanar within $\pm 20^\circ$ in each of the calorimeters. Studies with a single arm trigger showed that the trigger efficiency was essentially 100%. As in our previous analysis [2] the selected events had energy greater than 0.65 E_{beam} in each calorimeter and azimuthal angle of the shower centroid greater than 8° from the vertical axis.

Several sources of systematic error were reduced in the 1992 data. The geometrical definition of the masks was more precisely known and the events with spurious high energy deposits were eliminated. In addition, the use of the silicon tracker [2] allowed the acceptance borders of the unmasked calorimeter to be more precisely defined. The systematic uncertainty on the accepted cross section was estimated to be $\pm 0.38\%$. This is lower than the $\pm 0.5\%$ uncertainty of the 1991 luminosity and contains a component of $\pm 0.31\%$ in common with it, and with that of 1990.

The theoretical cross section was calculated on the basis of detailed simulations using the event generator BHLUMI [6] and the uncertainty was taken to be 0.25%. The total experimental and theoretical uncertainty on the luminosity is estimated to be $\pm 0.46\%$, containing a component of $\pm 0.40\%$ in common with that of 1991 and of 1990.

The Very Small Angle Tagger (VSAT), which covers the polar angle region 5 to 7 mrad, was used in the on-line monitoring and for consistency checks. It was not used in the luminosity measurement, since the determination of the absolute acceptance was less precise.

4 Hadronic Event Selection and Cross Section

As in our previous analysis [2] the hadronic event selection was based on charged particle tracks only. These were required to have a momentum greater than 0.4 GeV and a polar angle between 20° and 160°. For an event to be accepted, the charged multiplicity, N_{ch}, was required to be greater than 4 and the charged energy, E_{ch}, greater than 12% of the centre–of–mass energy. However, because of more efficient track reconstruction in the forward region, an additional selection was necessary to reduce the background from the e^+e^- channel. For events with N_{ch} less than 11, it was required that

$$\sqrt{E_{forw}^2 + E_{back}^2} < 0.9 \; E_{beam},$$

where E_{forw} and E_{back} are respectively the energies recorded in the forward and backward sections of the FEMC electromagnetic calorimeter. With this condition about 0.3% of the selected events were rejected, whereas simulation indicates that only 0.04% of $e^+e^- \to q\bar{q}$ would be rejected. The uncertainty due to this selection is estimated to be $\pm 0.02\%$.

The selection efficiency determined from simulation was $(95.00 \pm 0.11)\%$. The uncertainty was reduced compared to our previous analysis [2] by using the JETSET 7.3 parton shower generator [7] with different sets of tuning parameters. The trigger efficiency was determined from the data by comparing sets of independent triggers and was found to be greater than 99.99%.

The significant backgrounds are from $e^+e^- \to \tau^+\tau^-, e^+e^-$ and two-photon events. The τ background was estimated by comparing various distributions (e.g. thrust, charged energy, invariant masses per hemisphere[†]) of the selected data for low multiplicities (N_{ch} less than 9) to the corresponding ones from simulation of $q\bar{q}$, $\tau^+\tau^-$ and e^+e^- events. The $\tau^+\tau^-$ background was found to be $(0.58 \pm 0.05)\%$. The background from e^+e^- final states was estimated from simulation using the BABAMC generator [8] to be $(0.06 \pm 0.02\%)$. The two-photon background was found to be 13 ± 4 pb based on simulation using a generator including quark-parton, QCD and vector dominance contributions [9]. Other backgrounds such as $\mu^+\mu^-$ events, beam-gas or beam-wall interactions and cosmic showers were negligible (less than 0.5×10^{-4}).

A total of 696,543 events was selected, corresponding to an integrated luminosity of 23.955 pb^{-1}. The overall uncertainty of the hadronic selection amounts to 0.13%, of which 0.08% are common to the uncertainties of the 1990 and 1991 analyses [2].

The resulting cross section over 4π solid angle is:

$$\sigma_h = 30.440 \pm 0.053\ (stat.) \pm 0.040\ (syst.)\ \text{nb}.$$

The systematic uncertainty does not include the contribution from the luminosity measurement. This result is shown in Figure 1 together with previously published DELPHI results[2], and compared with the 5–parameter fit described in Section 6.

The event samples, acceptances, efficiencies, backgrounds and systematic errors in the hadronic cross section of the 1992 data are summarized in Table 1 together with the same quantities for the leptonic cross sections, and the leptonic forward–backward asymmetries.

5 Leptonic Event Selections, Cross Sections and Forward–Backward Charge Asymmetries

Cross sections and forward–backward asymmetries were determined in the channels e^+e^-, $\mu^+\mu^-$ and $\tau^+\tau^-$ as well as in the inclusive lepton channel. In general the techniques were similar to those used in our previous analysis [2], but any differences are pointed out in the following Sections.

5.1 The e^+e^- Channel

As in Ref. [2], two different methods of event selection were used in order to increase the overall efficiency and to allow a better determination of systematic uncertainties. In each method, both the electron and the positron were required to be within the range

[†] In this paper, hemispheres are defined by a plane perpendicular to the thrust axis.

$44^\circ < \theta < 136^\circ$, where θ is the polar angle of the particle with respect to the direction of the electron beam, and the acollinearity was required to be smaller than 10°.

In method 1, the selection relied on large energy deposits in the barrel electromagnetic calorimeter (HPC) and low charged multiplicity as indicated by the tracking detectors. Events from the reaction $e^+e^- \to \gamma\gamma$ were completely eliminated by the requirement of hits in the VD consistent with a final state containing at least one charged particle per hemisphere. The efficiency of this selection was determined from a sample of simulated events produced using the BABAMC [8] generator and was found to be $(89.42 \pm 0.38)\%$ in the θ acceptance region. This loss is mainly due to the fiducial cuts of the regions in azimuthal angle where the HPC has gaps between modules.

In method 2, two independent selections were used, one relying on the VD and the HPC and the second using information from the tracking detectors (other than VD), including ionization information from the TPC and the hit patterns in the OD. After correction for background, the efficiency of each selection and of the logical OR of the two could be determined from the data, the latter being found to be $(97.26 \pm 0.35)\%$ in the θ acceptance region. Both efficiencies do not include the loss due to the exclusion of the 4° polar angle region around 90° which amounted to 4.4%, as computed using two independent programs ALIBABA[10] and TOPAZ0 [11].

The trigger efficiency was determined from the data by comparing sets of independent triggers and was found to be greater than 99.99%.

The only significant background in each selection came from $\tau^+\tau^-$ events and was estimated by simulation using the KORALZ [12] generator. It was $(1.55 \pm 0.05)\%$ and $(1.23 \pm 0.04)\%$ for method 1 and method 2 respectively. After correction for backgrounds and efficiencies the two methods gave consistent results and the arithmetic mean of the two was used.

A total of 21,351 e^+e^- events were used in the method 2 analysis. This yielded a cross section in the angular range $44^\circ < \theta < 136^\circ$ and with an acollinearity less than 10° of

$$\sigma_e \text{ (s+t)} \;=\; 1.0436 \pm 0.0072\ (stat.) \pm 0.0036\ (syst.) \text{ nb.}$$

In order to allow fitting of the results by the ZFITTER [13] package, the t-channel exchange and its interference must be subtracted, and the accepted polar angle must be defined by the electron only. Corrections for both effects were computed using the programs ALIBABA[10] and TOPAZ0 [11]. After these corrections the s-channel cross section in the angular range $44^\circ < \theta < 136^\circ$ was found to be

$$\sigma_e \text{ (s-only)} \;=\; 0.9182 \pm 0.0072\ (stat.) \pm 0.0054\ (syst.) \text{ nb.}$$

The systematic error does not include the error due to the luminosity and it has a component of 0.0038 nb common to the data of 1990 and 1991.

The sample of events used for the cross section measurements was also used to determine the forward–backward asymmetry. In this analysis a new method has been used to determine the particle charge, based on the difference in azimuth between the VD track and the most energetic HPC cluster in the same hemisphere. With this method the ambiguous events (i.e. those having two tracks with the same sign or having a number of tracks different from two in the TPC) could be resolved, and the effects of possible wrong charge assignments on the asymmetry result were evaluated as being ± 0.0022. Another contribution to the systematic error on the asymmetry was due to the acceptance definition and was estimated to be ± 0.0011. The e^+e^- asymmetry in the angular range $44^\circ < \theta < 136^\circ$ was found to be

$$\mathrm{A}^e_{\mathrm{FB}} \text{ (s+t)} \;=\; 0.1177 \pm 0.0069\ (stat.) \pm 0.0025\ (syst.).$$

Correcting for the t-channel and interference effects, and for the requirement that only the electron be in the acceptance, the s-channel e^+e^- asymmetry in the angular range $44° < \theta < 136°$ was deduced to be

$$A_{FB}^{e} \text{ (s-only)} \quad = \quad 0.0206 \pm 0.0079 \ (stat.) \pm 0.0030 \ (syst.).$$

The systematic error includes effects due to the LEP energy and the t-channel subtraction, and contains a component of 0.0024 in common with the data of 1990 and 1991.

5.2 The $\mu^+\mu^-$ Channel

The selection procedure for the $e^+e^- \to \mu^+\mu^-$ candidates was similar to that described in Ref. [2]. The polar angle range for the determination of the cross section was $20° < \theta < 160°$. Events were required to have two charged particles each of momentum greater than 15 GeV, and with maximum acollinearity increased to 20°. It was required that each of the particles be identified as a muon. Identification was achieved by requiring associated hits in the muon chambers MUB or MUF, or by energy depositions in the hadron calorimeter HCAL, or the electromagnetic calorimeters HPC or FEMC, consistent with a minimum ionizing particle. A total of 31,044 events passed these selections. The inefficiency of the event selection due to the tracking detectors was estimated from the data itself, supplemented by the study of a sample of simulated events produced using the DYMU3 [14] generator. The muon identification efficiency was determined directly from the data. The overall event selection and identification probability was found to be $(94.63 \pm 0.30)\%$. The trigger efficiency was computed by comparing sets of independent triggers and was found to be $(99.87 \pm 0.08)\%$.

The significant backgrounds were from the $\tau^+\tau^-$ final state and from cosmic rays. The $\tau^+\tau^-$ background was determined from Monte Carlo simulation using the KORALZ [12] generator, and also by studying variables in the data which are sensitive to this background. It was found to be $(2.00 \pm 0.20)\%$ in the selected sample. The cosmic ray background was determined by studying events which originated close to the interaction point, but outside the limits allowed for selected events, and was found to be $(0.15 \pm 0.05)\%$.

After subtraction of backgrounds and correction for inefficiencies, the cross section for the events in which the negative muon was in the angular range $20° < \theta < 160°$ and with the cuts on momenta and acollinearity given above was found to be

$$\sigma_\mu \quad = \quad 1.3450 \pm 0.0076 \ (stat.) \pm 0.0054 \ (syst.) \text{ nb}.$$

The systematic error does not include that due to the luminosity and is common to the data of 1990 and 1991.

For the asymmetry measurement, the angular range was extended to $11° < \theta < 169°$ since an absolute normalization was not required. With the same cuts on momenta and acollinearity as for the cross section, 32,382 events were selected. By simulation it was estimated that the sample contained a background of $(2.00 \pm 0.20)\%$ of $\tau^+\tau^-$ events, however these do not bias the asymmetry. A cosmic ray study similar to the one used for the cross section showed that the sample contained $(0.14 \pm 0.05)\%$ background from this source, but with a negligible effect on the asymmetry. Significant systematic errors arising from asymmetries in the detector, from the measurement of polar angle and from possible angle–dependent momentum acceptances, were determined from the data and were found to give an overall systematic error of ± 0.0010, which can be considered as common to the data of 1990 and 1991. The asymmetry, corrected to the full angular

range, but not for the momenta and acollinearity cuts was determined by a maximum likelihood fit to the lowest order form of the angular distribution, and was found to be

$$A_{FB}^{\mu} = 0.0056 \pm 0.0053\ (stat.) \pm 0.0010\ (syst.).$$

5.3 The $\tau^+\tau^-$ Channel

The selection of tau pair candidates followed quite closely the analysis of the 1991 data sample described in reference [2] but with several important changes which are described below. The events were required to be of low multiplicity and to consist of two well isolated jets. The thrust axis, computed using both charged and neutral energy, had to lie in the polar angle interval $43^\circ < \theta < 137^\circ$ as did the highest momentum particle in at least one of the event hemispheres. Furthermore, events were rejected if the highest momentum particle in both hemispheres were reconstructed in the polar angle interval $88^\circ < \theta < 92^\circ$, where the track reconstruction efficiency is not well modelled by the detector simulation. A new feature of this analysis was the reconstruction of photons which converted before the TPC. The effect of this was to increase the number of tau pairs which satisfied the charged particle multiplicity and jet isolation requirements after the conversion pair tracks were replaced with a photon of the appropriate energy.

The radial momentum variable P_{rad} (defined as $P_{rad} = \sqrt{P_1^2 + P_2^2}/P_{beam}$, with P_1 and P_2 the momenta of the highest momentum charged particle in each hemisphere) and the radial energy E_{rad} (defined as $E_{rad} = \sqrt{E_1^2 + E_2^2}/E_{beam}$ where E_1 and E_2 are the energies deposited in the electromagnetic calorimeters inside a 30° half-angle cone around the direction of the thrust axis in each hemisphere) were both required to be less than some maximum allowed value which depended on several other features of the event. The radial momentum had only to be less than unity (as in the analysis of the 1991 data) if the event was consistent with being a muon pair by requiring that the highest momentum particle in at least one of the hemispheres satisfied very similar muon identification criteria to those described in the Section 5.2 above. This removes a systematic bias in the determination of the background from $e^+e^- \to e^+e^-$ events due to the difficulty in precisely simulating the momentum spectrum of high energy electrons in the detector. The radial energy selection depended on the proximity of the highest momentum particle in each hemisphere to the boundaries between adjacent HPC modules (at intervals of 15° in azimuthal angle), where a substantial fraction of the deposited energy was lost. If the entry point of the extrapolated trajectories of both these particles was more than 1.5° from the nearest boundary then the radial energy was required to be less than 0.9, otherwise it had to be less than 0.6. This requirement was more severe than in the analysis of the 1991 data [2] because the radial momentum selection was no longer effective in eliminating the $e^+e^- \to e^+e^-$ events from the tau pair sample.

These cuts efficiently removed most of the potential backgrounds from hadronic Z^0 decays, two-photon events, $\mu^+\mu^-$ and e^+e^- events. Cosmic ray, beam-gas and beam-wall events were removed with tight cuts on the impact parameters of tracks relative to the average interaction point. A total of 16,919 events were selected for the cross section and asymmetry measurement.

The tau pair selection efficiency was determined from Monte Carlo simulated data produced using the KORALZ [12] generator. After applying a small correction for the imperfect modelling of the loss of charged particles in the azimuthal dead regions of the TPC and a small smearing of the Monte Carlo momentum and HPC energy distributions, the selection efficiency, defined as the number of events selected divided by the total

number of tau pairs generated in 4π solid angle, was $(48.01 \pm 0.16)\%$, where the error quoted is solely due to the Monte Carlo statistics. The trigger efficiency was calculated by examining a set of independent trigger components and found to be $(99.98 \pm 0.01)\%$.

The most significant contributions to the systematic error on the tau pair selection efficiency are the TPC track loss correction, the smearing of the Monte Carlo momentum, the HPC energy response and the radial momentum and energy cuts. Other smaller sources of systematic errors are the choice of the radial impact parameter cuts, the effect of identifying converted photons, and the tau polarisation and branching ratio values used in the event generator. The total error on the cross section from the selection efficiency determination was 0.58%, which includes the Monte Carlo statistical error.

All backgrounds were estimated using Monte Carlo simulations. The various corrections and smearings to the Monte Carlo samples described above were taken into account in these computations. The background samples were generated with BABAMC [8] (e^+e^-), DYMU3 [14] ($\mu^+\mu^-$), JETSET 7.3 Parton Shower [7] ($q\bar{q}$) and the generator of ref [9] for the two-photon processes. By applying the tau pair selection cuts to the simulated data the resonant backgrounds from e^+e^-, $\mu^+\mu^-$ and hadronic final states were observed to be $(1.14\pm0.15)\%$, $(0.46\pm0.07)\%$ and $(0.84\pm0.15)\%$ respectively of the selected tau pair sample. The non-resonant 2-photon background was estimated to be 3.3 ± 0.9 pb, with the dominant contributions coming from $e^+e^- \to e^+e^-e^+e^-$ and $e^+e^- \to e^+e^-\mu^+\mu^-$. The residual cosmic ray background was estimated to be $(0.11 \pm 0.05)\%$. The total error on the cross section due to the background subtraction was 0.26% and the overall systematic error on the cross section was 0.63%.

After subtraction of the backgrounds and correction for selection efficiency, the cross section in 4π solid angle was found to be

$$\sigma_\tau \;=\; 1.491 \pm 0.012\ (stat.) \pm 0.009\ (syst.)\ \text{nb}.$$

The systematic error does not includes that due to the luminosity and includes a component of 0.007 nb common to the data of 1990 and 1991.

The asymmetry analysis was carried out in the same polar angle range as the cross-section. The forward or backward scattered events were defined using the polar angle of the thrust axis and the charge sum of particles in each hemisphere. There were 231 (228) events in which the charge sum in both hemispheres was positive (negative) and these were discarded from the asymmetry measurement. Finally, 369 events which did not belong to the 1–N (N=1,2,3,4,5) or 3–3 topologies were rejected since the hemisphere charge determination in these cases was not reliable (the numbers defining the topologies refer to the number of charged particles in each hemisphere). The forward-backward asymmetry, calculated by the maximum likelihood method using the lowest order form of the angular distribution, taking into account the angular distribution of the background, was found to be

$$\mathrm{A}^\tau_{\mathrm{FB}} \;=\; 0.0092 \pm 0.0088\ (stat.) \pm 0.0017\ (syst.),$$

corresponding to 4π solid angle. The systematic error includes the uncertainty on the e^+e^- subtraction, the contribution from the charge misidentification probability determined from the number of like-sign tau pairs and the estimate of the effect of neglecting QED radiative corrections to the fitted angular distribution. A component of 0.0010 of the systematic error is common to the published 1990 and 1991 data.

5.4 The Inclusive Lepton Channels

As in our previous analysis [2] a flavour independent analysis was carried out in order to provide a cross–check on the leptonic analyses described above. The event selection procedure was the same as for the 1991 data, that is, events were required to have between 2 and 6 charged particles with momentum greater than 0.2 GeV, with at least two lying in the polar angle range $43° < \theta < 137°$. At least one hemisphere was required to contain one charged particle, and the other between 1 and 5 charged particles. The acollinearity, defined by the isolated track and the resultant momentum of the group of particles in the other hemisphere, was required to be less than 20° and one particle in the event was required to have momentum greater than 3 GeV. A total of 65,200 events was selected.

For e^+e^- and $\mu^+\mu^-$ within the accepted polar angle range, the selection inefficiency was determined principally by two sources: loss of those particles passing through insensitive regions of the TPC, and failure to reconstruct a particle passing through the sensitive region. Both of these effects were measured from the data using events identified as being of these types. The dead regions of the TPC were found to give a track inefficiency of $(4.87 \pm 0.14)\%$. Within the sensitive region the track loss was found to be $(0.30 \pm 0.20)\%$ for muons and $(0.86 \pm 0.20)\%$ for electrons. The overall selection efficiencies were therefore $(94.83 \pm 0.24)\%$ for $\mu^+\mu^-$ events and $(94.27 \pm 0.24)\%$ for e^+e^- events.

For the $\tau^+\tau^-$ channel a sample of Monte Carlo events produced using the generator KORALZ [12] was used to determine the efficiency. The result was an event selection efficiency of $(57.40 \pm 0.43)\%$, corresponding to events over the full solid angle.

The trigger efficiency was taken as the average of those determined for the flavour separated channels, weighting by the estimated number of events of each type in the selected sample. It was found to be $(99.95^{+0.05}_{-0.10})\%$.

The significant sources of background were from cosmic rays, from two-photon processes and from hadronic decays. The cosmic ray background was estimated from the distribution of impact parameters within the data and was found to be $(0.52 \pm 0.03)\%$. The other backgrounds were estimated from simulated samples. The cross section for two-photon processes within the acceptance was found to be 5.8 ± 0.3 pb and the background from hadronic decays was estimated to be $(0.14 \pm 0.02)\%$.

The t-channel contribution in the e^+e^- channel was subtracted in a similar manner to that described in Section 5.1, taking account of the fraction of e^+e^- events in the sample. The corresponding uncertainty was estimated to be $\pm 0.05\%$.

After subtracting backgrounds and correcting for selection efficiencies, the s-channel cross section for one flavour was found to be over 4π solid angle:

$$\sigma_l \;=\; 1.4938 \pm 0.0059\ (stat.) \pm 0.0045\ (syst.)\ \text{nb}.$$

The systematic error does not includes that due to the luminosity, and is common to the data of 1990 and 1991.

For the determination of the forward–backward asymmetry, only the events of the 1–1 topology, and having two particle tracks of opposite charge were used. A sample of 50,356 events was obtained. The asymmetry was computed by the counting method and corrections were applied for cosmic ray and two-photon backgrounds. The asymmetry due to the t-channel contribution in e^+e^- was estimated as in Section 5.1, taking into account the fraction of e^+e^- events in the 1–1 topology. Correcting to the full angular range, the asymmetry is found to be

$$\mathrm{A}^l_{\mathrm{FB}} \;=\; 0.0175 \pm 0.0037\ (stat.) \pm 0.0025\ (syst.),$$

where the systematic error comes mainly from the t-channel subtraction and possible charge misidentification, and is common to that of the 1990 and 1991 data.

The inclusive lepton results were compared with those of the analyses with lepton identification. To do this the lepton–identified results were corrected, using ZFITTER [13], so that they corresponded to a 4π detector with no cuts applied. The weighted mean of the lepton–identified results was then computed. The ratio of the measured cross section for $e^+e^- \to l^+l^-$ to the mean of the lepton–identified results was then found to be 0.9972 ± 0.0052, where the error takes account of the systematic errors, and statistical errors due the incomplete overlap of the different channels. Similarly the difference in the inclusive lepton and the mean of the lepton–identified results for the forward–backward asymmetry was found to be -0.0075 ± 0.0055. The good agreement supports the validity of the lepton–identified results.

	Hadrons	e^+e^-	$\mu^+\mu^-$	$\tau^+\tau^-$	l^+l^-
Cross section					
θ acceptance (°)	0-180	44-136	20-160	43-137	43-137
Selected events	696,543	21,351	31,044	16,919	65,200
Selection efficiency (%)	95.00 ± 0.11	97.26 ± 0.35	94.63 ± 0.30	81.71 ± 0.47	92.65 ± 0.27
Trigger efficiency (%)	> 99.99	> 99.99	99.87 ± 0.08	99.98 ± 0.01	$99.95^{+0.05}_{-0.10}$
$\tau^+\tau^-$ background (%)	0.58 ± 0.05	1.23 ± 0.04	2.00 ± 0.20	–	–
$q\bar{q}$ background (%)	–	–	–	0.84 ± 0.15	0.14 ± 0.02
$e^+e^- + \mu^+\mu^-$ bkgd. (%)	0.06 ± 0.02	–	–	1.60 ± 0.17	–
Two-photon bkgd. (pb)	13 ± 4	–	–	3.3 ± 0.9	5.8 ± 0.6
Cosmic ray bkgd. (%)	–	–	0.15 ± 0.05	0.11 ± 0.05	0.52 ± 0.03
Tot. syst. error (%)	± 0.13	$\pm 0.59^\dagger$	± 0.37	± 0.63	± 0.30
Asymmetry A_{FB}^f					
θ acceptance (°)	–	44-136	11-169	43-137	43-137
Selected events		21,351	32,382	16,091	50,356
Tot. syst. error	–	$\pm 0.0030^\dagger$	± 0.0010	± 0.0017	± 0.0025

Table 1: Summary of event samples, angular acceptances, efficiencies within the acceptances, backgrounds and systematic errors in the hadronic and leptonic cross sections, and the leptonic forward–backward asymmetries for the 1992 data. The e^+e^- data refer specifically to analysis method 2. The total systematic uncertainty of $\pm 0.46\%$ in the luminosity is not included in the above numbers.
†Includes the uncertainty due to the t-channel subtraction.

The cross section and forward–backward asymmetry results for the leptonic channels are shown in Figures 2 and 3 respectively, together with previously published DELPHI results[2], and with the results of the 5–parameter fit described in Section 6.

6 Z^0 Parameters

Fits to the hadronic cross sections and the leptonic cross sections and forward–backward asymmetries of 1990, 1991 and 1992, were made using the program ZFITTER [13]. Full account was taken of the LEP energy uncertainties and their point-to-point

correlations [1]. The overall energy scale of the 1990 data was assigned an uncertainty of 26 MeV [2]. The energies of the 1991 data were obtained by the procedures described in ref. [2]. The single centre-of-mass energy of the 1992 data was assigned an uncertainty of 18 MeV [3], uncorrelated to that of the other years. If independent couplings are allowed for the different lepton species then a 9-parameter fit yields the following parameters :

$$\begin{aligned}
M_{\mathrm{Z}} &= 91.187 \pm 0.009 \text{ GeV} \\
\Gamma_{\mathrm{Z}} &= 2.483 \pm 0.012 \text{ GeV} \\
\sigma_0 &= 41.23 \pm 0.20 \text{ nb} \\
R_e &= 20.74 \pm 0.18 \\
R_\mu &= 20.54 \pm 0.14 \\
R_\tau &= 20.68 \pm 0.18 \\
\mathrm{A}_{\mathrm{FB}}^{\mathrm{o}\ e} &= 0.025 \pm 0.009 \\
\mathrm{A}_{\mathrm{FB}}^{\mathrm{o}\ \mu} &= 0.014 \pm 0.005 \\
\mathrm{A}_{\mathrm{FB}}^{\mathrm{o}\ \tau} &= 0.022 \pm 0.007 \\
\chi^2/DF &= 108/104,
\end{aligned}$$

where M_{Z}, Γ_{Z} and σ_0 are respectively the mass and width of the Z^0 and the hadronic pole cross section. The parameters R_f for lepton species f are defined as

$$R_f = \frac{\Gamma_{\mathrm{had}}}{\Gamma_f},$$

where Γ_{had} and Γ_f are the partial decay widths into hadrons and the lepton species f respectively. The parameters $\mathrm{A}_{\mathrm{FB}}^{\mathrm{o}\ f}$ are defined as:

$$\mathrm{A}_{\mathrm{FB}}^{\mathrm{o}\ f} = 3\frac{g_{V_e} g_{A_e}}{(g_{V_e}^2 + g_{A_e}^2)} \frac{g_{V_f} g_{A_f}}{(g_{V_f}^2 + g_{A_f}^2)},$$

where g_{V_f} and g_{A_f} are effective vector and axial-vector couplings. The correlation coefficients for the parameters of the 9-parameter fit are given in Table 2.

These fit parameters are in good agreement with the hypothesis of lepton universality of the couplings. This is demonstrated in Figure 4 where the allowed regions of $\mathrm{A}_{\mathrm{FB}}^{\mathrm{o}\ f}$ and R_f for each lepton species are shown, together with some predictions of the Standard Model. A 5–parameter fit assuming flavour independence of the couplings was therefore carried out and yielded the following results:

$$\begin{aligned}
M_{\mathrm{Z}} &= 91.187 \pm 0.009 \text{ GeV} \\
\Gamma_{\mathrm{Z}} &= 2.483 \pm 0.012 \text{ GeV} \\
\sigma_0 &= 41.23 \pm 0.20 \text{ nb} \\
R_l &= 20.62 \pm 0.10 \\
\mathrm{A}_{\mathrm{FB}}^{\mathrm{o}} &= 0.0177 \pm 0.0037 \\
\chi^2/DF &= 110/108.
\end{aligned}$$

The correlation coefficients of the parameters of the 5-parameter fit are given in Table 3. Here R_l is defined for the Z^0 decay into a pair of massless charged leptons and is treated consistently throughout.

Alternatively the results of the preceeding fits can be expressed in terms of the following parameters:

$$\begin{aligned}
\Gamma_e &= 83.31 \pm 0.54 \text{ MeV} \\
\Gamma_\mu &= 84.15 \pm 0.77 \text{ MeV} \\
\Gamma_\tau &= 83.55 \pm 0.91 \text{ MeV} \\
\Gamma_l &= 83.56 \pm 0.45 \text{ MeV} \\
g^2_{V_l} &= (1.50 \pm 0.31) \times 10^{-3} \\
g^2_{A_l} &= 0.2499 \pm 0.0014 \\
\Gamma_{\rm inv} &= 509.4 \pm 7.0 \text{ MeV} \\
\Gamma_{\rm had} &= 1.723 \pm 0.010 \text{ GeV},
\end{aligned}$$

where Γ_l, g_{V_l}, g_{A_l} and $\Gamma_{\rm inv}$ are defined assuming lepton universality, and $\Gamma_{\rm inv}$ is the partial width for Z^0 decays into invisible final states.

The results of the 5–parameter and 9–parameter fits to the DELPHI data are in good agreement with those published by the other LEP collaborations [15–17].

	$\Gamma_{\rm Z}$	σ_0	R_e	R_μ	R_τ	$A^{0,e}_{\rm FB}$	$A^{0,\mu}_{\rm FB}$	$A^{0,\tau}_{\rm FB}$
$M_{\rm Z}$	-0.01	0.01	0.01	0.01	0.00	0.00	0.07	0.08
$\Gamma_{\rm Z}$		-0.14	0.00	0.00	0.00	0.00	0.00	0.00
σ_0			0.07	0.10	0.07	0.00	0.00	-0.01
R_e				0.05	0.04	0.01	0.00	0.00
R_μ					0.05	0.00	0.01	0.00
R_τ						0.00	0.00	0.01
$A^{0,e}_{\rm FB}$							0.03	0.02
$A^{0,\mu}_{\rm FB}$								0.04

Table 2: The correlation coefficients for the parameters of the 9-parameter fit.

	$\Gamma_{\rm Z}$	σ_0	R_l	$A^0_{\rm FB}$
$M_{\rm Z}$	-0.01	0.01	0.00	0.16
$\Gamma_{\rm Z}$		-0.14	0.00	-0.01
σ_0			0.13	-0.01
R_l				0.01

Table 3: The correlation coefficients for the parameters of the 5-parameter fit.

7 Interpretation of the Results within the Standard Model

Within the Minimal Standard Model the ratio Γ_ν/Γ_l shows little dependence on the unknown parameters. Taking the mass of the top quark, m_t, as 180 GeV and the mass

of the Higgs boson, m_H, as 300 GeV the model predicts

$$\Gamma_\nu/\Gamma_l \;=\; 1.992 \pm 0.002,$$

where the uncertainty corresponds to variations of m_t and m_H within the ranges 130 GeV $< m_t <$ 230 GeV and 60 GeV $< m_H <$ 1000 GeV respectively. From the results given in Section 6 the ratio

$$\Gamma_{\rm inv}/\Gamma_l \;=\; 6.10 \pm 0.08$$

can be derived, and hence the number of light neutrino species can be deduced to be

$$\mathrm{N}_\nu \;=\; 3.060 \pm 0.041.$$

An alternative procedure is to carry out a Standard Model fit, but leaving the number of neutrino species and the value of the strong coupling constant, $\alpha_{\rm s}$, free. The results were:

$$\begin{aligned} \alpha_{\rm s} &= 0.098 \pm 0.014 \\ \mathrm{N}_\nu &= 3.057 \pm 0.040. \end{aligned}$$

If the value for the strong coupling constant $\alpha_{\rm s}$ as determined by the DELPHI collaboration [18],

$$\alpha_{\rm s} \;=\; 0.123 \pm 0.005$$

was used as a constraint then the result:

$$\mathrm{N}_\nu \;=\; 3.023 \pm 0.035,$$

was obtained. If the number of neutrino species was fixed to be three, but $\alpha_{\rm s}$ was left unconstrained, then the fit yielded the value:

$$\alpha_{\rm s} \;=\; 0.108 \pm 0.012.$$

If the weak mixing angle is defined by the relation

$$g_{V_l}/g_{A_l} \;=\; (1 - 4\sin^2\theta_{eff}^{lept}),$$

then the leptonic vector and axial-vector couplings correspond to

$$\sin^2\theta_{eff}^{lept} \;=\; 0.2306 \pm 0.0020.$$

A Standard Model fit to all the cross section and asymmetry data using the value of $\alpha_{\rm s}$ measured by the DELPHI collaboration [18] as a constraint, yields the following value for the top quark mass:

$$m_t \;=\; 157^{+36}_{-48}(expt.)^{+19}_{-20}(Higgs)\ \text{GeV},$$

where $(Higgs)$ represents the variation due to Higgs boson mass in the range 60 to 1000 GeV, with central value 300 GeV. This value of m_t corresponds to:

$$\sin^2\theta_{eff}^{lept} \;=\; 0.2328 \pm 0.0013(expt.)^{+0.0001}_{-0.0003}(Higgs)$$

8 Summary

During 1992, DELPHI accumulated approximately 24 pb^{-1} at the Z^0 peak. These data have been analysed to give hadronic and leptonic cross sections and leptonic forward-backward asymmetries, all at a mean centre-of-mass energy of 91.280 GeV. These results have been combined with the previous DELPHI results at energies around the Z^0 peak to give improved determinations of the resonance parameters, notably the leptonic partial widths and couplings. The leptonic couplings correspond to a value of the weak mixing angle of

$$\sin^2\theta_{eff}^{lept} \quad = \quad 0.2306 \pm 0.0020.$$

Within the context of the Standard Model the data can be used to determine the strong coupling constant α_s. We find $\alpha_s = 0.108 \pm 0.012$. If the value of α_s determined by the DELPHI collaboration from a study of hadronic final states is used as a constraint, then the Standard Model fit yields

$$m_t \quad = \quad 157^{+36}_{-48}(expt.)^{+19}_{-20}(Higgs) \text{ GeV}.$$

Acknowledgements

We thank the SL Division of CERN for the excellent performance of the LEP collider and for their careful work on the beam energy determinations. We are also grateful to the technical and engineering staffs in our laboratories and to our funding agencies for their continuing support.

References

[1] Working Group on LEP Energy and the LEP Collaborations, Phys. Lett. **B307** (1993) 187.

[2] DELPHI Collaboration, P. Abreu et al., "Measurements of the Lineshape of the Z^0 and Determination of Electroweak Parameters from its Hadronic and Leptonic Decays", preprint CERN-PPE/94-08, Nucl. Phys. **B** to be published.

[3] L. Arnaudon et al., "The Energy Calibration of LEP in 1992", CERN SL/93-21 (DI) (1993), unpublished.

[4] DELPHI Collaboration, P. Aarnio et al., Nucl. Instr. & Meth. **A303** (1991) 233.

[5] DELPHI Collaboration, "DELPHI Event generation and detector simulation - User guide", DELPHI Note 89-67 (1989), unpublished.

[6] S. Jadach et al., Comput. Phys. Commun. **70** (1992) 305.

[7] T. Sjöstrand, Comput. Phys. Commun. **27** (1982) 243, ibid.**28** (1983) 229.
T. Sjöstrand and M. Bengtsson, Comput. Phys. Commun. **43** (1987) 367.
T. Sjöstrand, "PYTHIA 5.6 JETSET 7.3 Physics and Manual", preprint CERN-TH 6488/92 (1992).

[8] F.A. Berends, W. Hollik and R.Kleiss, Nucl. Phys. **B304** (1988) 712.

[9] S. Nova, A. Olshevski and T. Todorov, "Monte Carlo event generator for two photon processes", DELPHI Note 90-35 (1990), unpublished,
F.A. Berends, P.H. Daverveldt, R. Kleiss, Comput. Phys. Commun. **40** (1986) 285, and Nucl. Phys. **B253** (1985) 441.

[10] W.J.P. Beenakker, F.A. Berends and S.C. van der Marck,
Nucl. Phys. **B349** (1991) 323.

[11] G. Montagna et al., Nucl. Phys. **B401** (1993) 3, and Comput. Phys. Commun. **76** (1993) 328.

[12] S. Jadach, B.F.L. Ward and Z. Was, Comput. Phys. Commun. **66** (1991) 276.

[13] D. Bardin et al., "ZFITTER: An Analytical Program for Fermion Pair Production in e^+e^- Annihilation", preprint CERN-TH 6443/92 (1992) and references therein.

[14] J.E. Campagne and R. Zitoun, Z. Phys. **C43** (1989) 469.

[15] ALEPH Collaboration, D. Buskulic et al., "Z production cross-sections and lepton pair forward-backward asymmetries", preprint CERN-PPE/94-30 (1994).

[16] L3 Collaboration, O. Adriani et al., "Results from the L3 Experiment at LEP", preprint CERN-PPE/93-31 (1993).

[17] OPAL Collaboration, R. Akers et al., Z. Phys. **C61** (1994) 19.

[18] DELPHI Collaboration, P. Abreu et al., Z. Phys. **C59** (1993) 21.

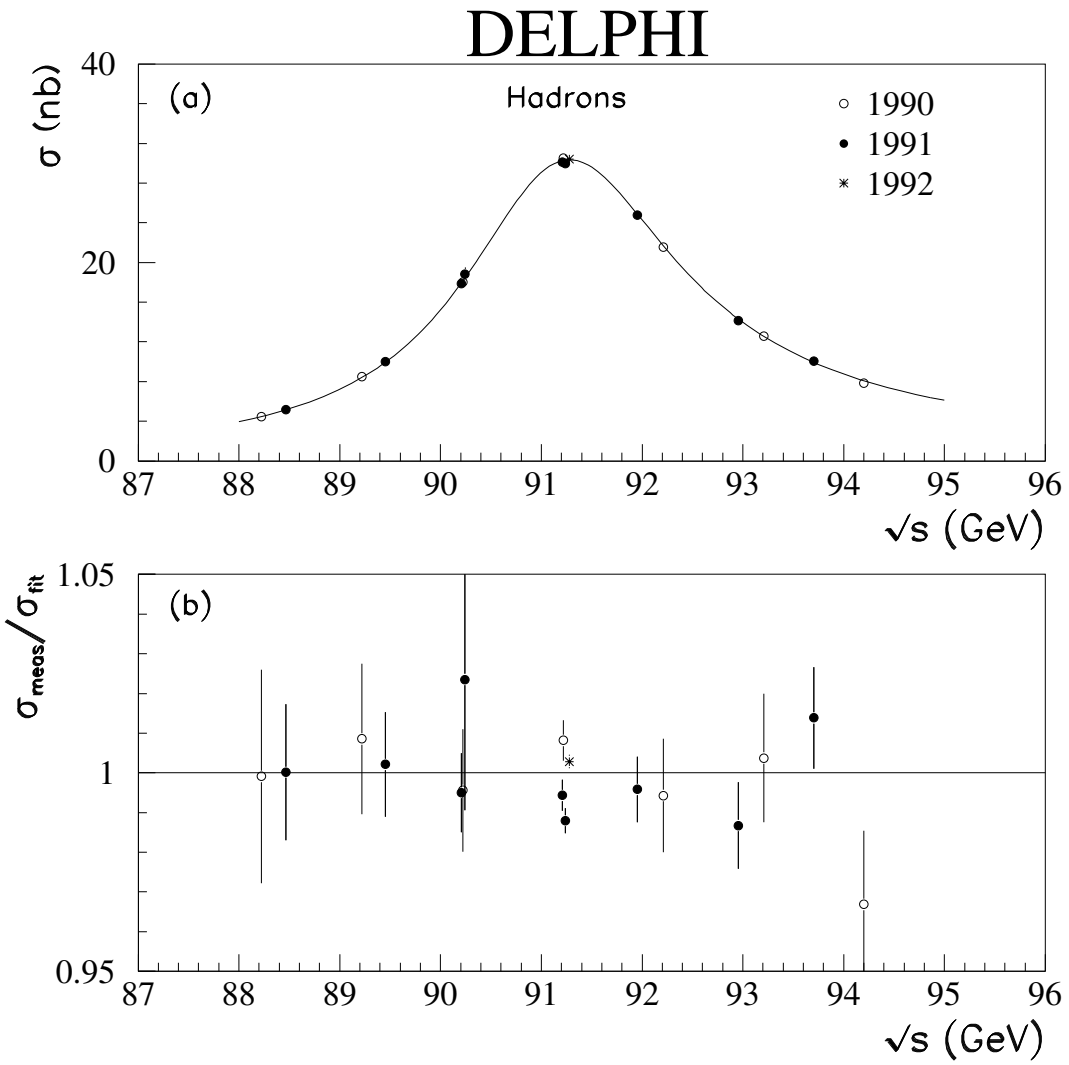

Figure 1: Hadronic cross sections from 1990, 1991 and 1992 data. The errors shown are statistical only. The uncorrelated systematic error between the 1990 and 1991 results amounts to 0.6% and that between the 1992 and 1990/91 results 0.30%. In (a) the data are shown together with the result of the 5-parameter fit described in Section 6. Plot (b) shows the ratio of the measurements to the best fit values.

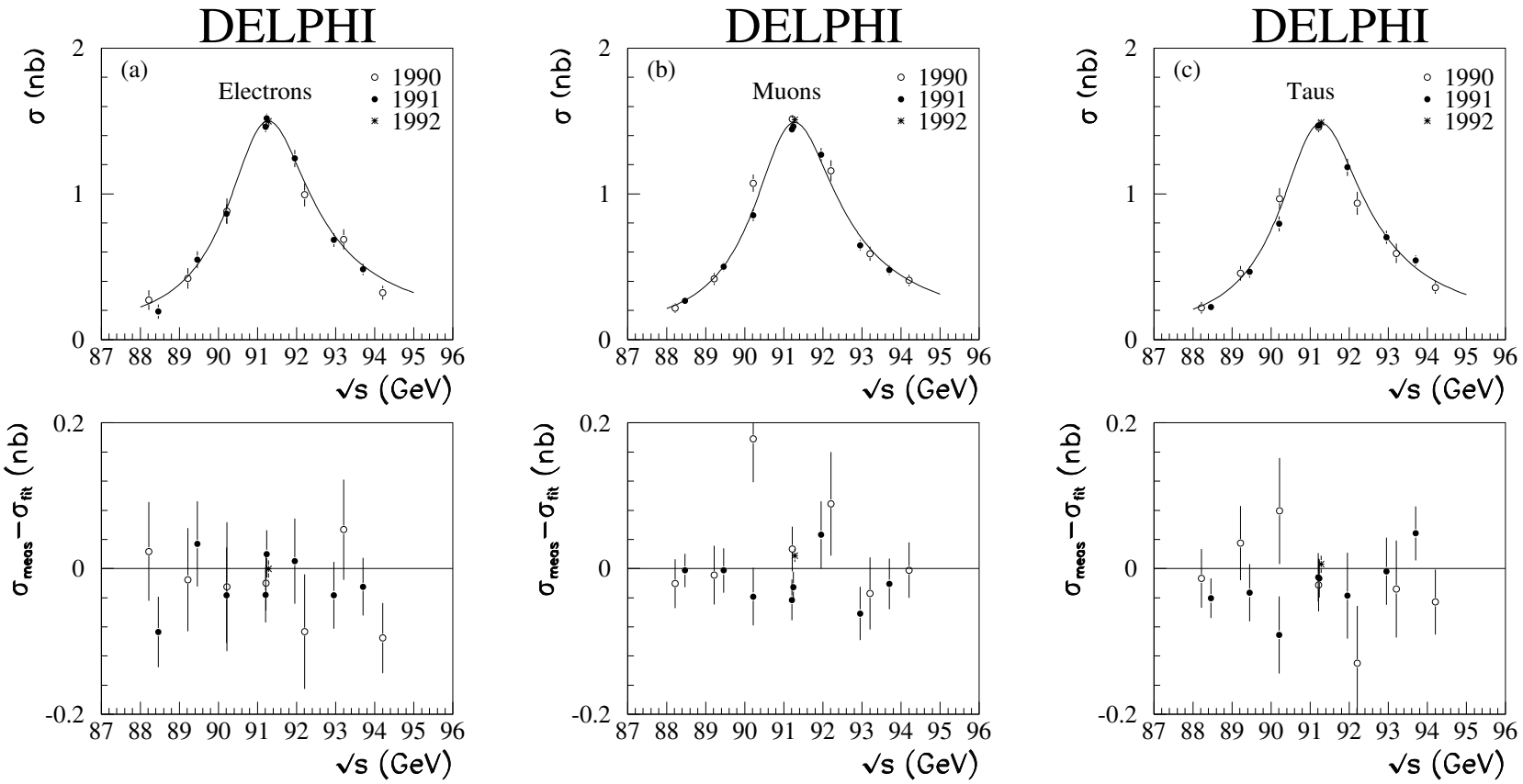

Figure 2: Cross sections in the (a) e^+e^-, (b) $\mu^+\mu^-$ and (c) $\tau^+\tau^-$ channels. The cross sections are extrapolated to the full solid angle and corrected for the acollinearity and momentum cuts. Only statistical errors are shown. The lower plots show the differences between the measured points and the best fit values. The curves are the results of the 5–parameter fit described in Section 6.

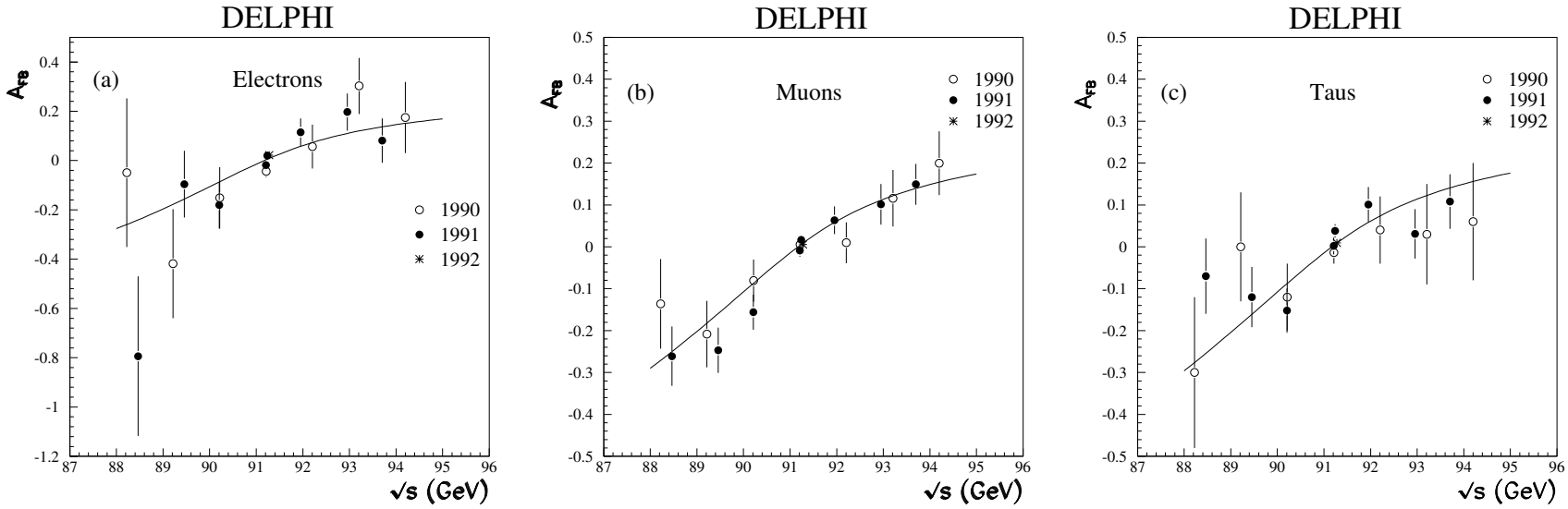

Figure 3: Forward–backward asymmetries in the (a) e^+e^-, (b) $\mu^+\mu^-$ and (c) $\tau^+\tau^-$ channels. The asymmetries are extrapolated to the full solid angle but not corrected for the acollinearity and momentum cuts. The curves are the results of the 5–parameter fit described in Section 6.

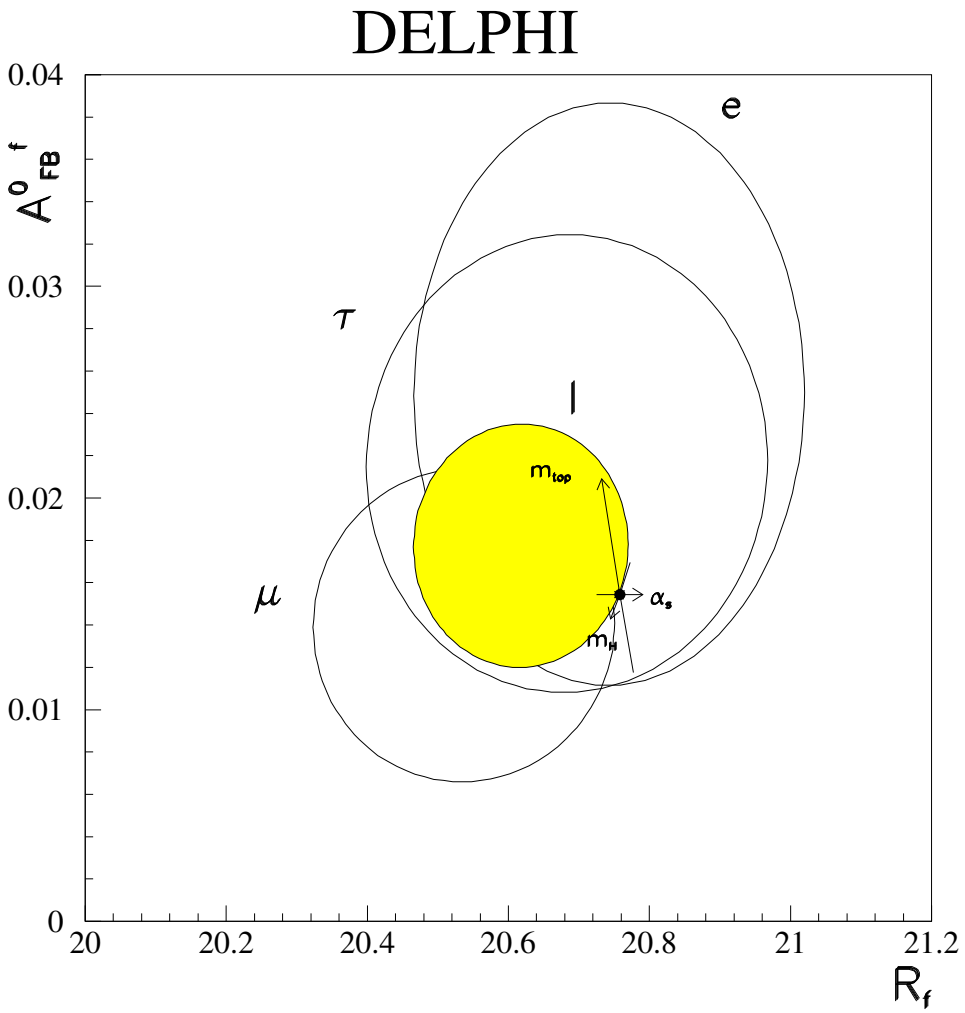

Figure 4: Allowed contours at the 68% confidence level in the $A^{0,f}_{FB}$ - R_f plane. The contours from the 9–parameter fit, without assuming lepton universality, are indicated by e, μ, and τ, while the region allowed by the 5–parameter fit assuming lepton universality is indicated by l and is shaded. The point shows the expectation of the Standard Model for $m_t = 180$ GeV, $\alpha_s = 0.123$ and $m_H = 300$ GeV. The arrows show the changes of the prediction as m_t varies from 100 GeV to 250 GeV, α_s from 0.118 to 0.128 and m_H from 60 GeV to 1000 GeV.